Sensors and Actuators A 270 (2018) 252–261

Contents lists available at ScienceDirect

Sensors and Actuators A: Physical

journal homepage: www.elsevier.com/locate/sna

Thin-film repulsive-force electrostatic actuators

Ethan W. Schaler[a], Tarek I. Zohdi[b], Ronald S. Fearing[a,*]

[a] Dept. of Electrical Engineering and Computer Sciences, University of California, Berkeley, CA 94720, USA
[b] Dept. of Mechanical Engineering, University of California, Berkeley, CA 94720, USA

ARTICLE INFO

Article history:
Received 11 August 2017
Received in revised form 6 December 2017
Accepted 21 December 2017
Available online 29 December 2017

Keywords:
Electrostatic actuator
Repulsive forces
Thin-films

ABSTRACT

We demonstrate thin-film repulsive-force electrostatic actuators that employ a new electrode pattern and are useful for low-force actuation applications. Compared to prior patterns, the new electrode geometry increases electrostatic force production by an order of magnitude (at equal voltages) and eliminates the most common shorting failure modes. These electrostatic actuators have stable open-loop operation with no pull-in instability, low mechanical hysteresis, and peak force in rest configurations. The actuators are fabricated with a planar, flex-circuit manufacturing process, allowing production at scale and over large areas. Two-layer out-of-plane linear actuators (25 × 10 mm electrode area) were characterized: with 0–1000 V inputs (40×10^6 V/m), blocked normal forces of 9.03 mN (36.1 Pa) were generated, and controllable linear displacements up to 511 μm were measured across an open loop bandwidth of 43 Hz. Finally, we present a 290 mg 1-DoF micro-mirror system for laser beam steering that employs a two-layer out-of-plane rotational actuator for open-loop stable operation with controlled angular displacements up to 5.1° at 1000 V/16 Hz.

1. Introduction

Advances in planar manufacturing have leveraged new processes and materials to develop a range of innovative robots and sensors [1–6]. Devices are composed of functional materials (films, fabrics, composites, inks, etc.) and use layering, patterning, folding, and bonding steps to form complex kinematic structures with integrated circuitry [3]. We apply these same standard manufacturing steps to fabricate thin-film repulsive-force electrostatic actuators.

Our initial goal is to produce cm-scale planar actuators, capable of generating mN forces and mm displacements at ∼30 Hz (video-compatible) frequencies, for applications in mobile robotics (i.e. a lightweight laser beam steering system) and beyond. Numerous viable actuator technologies exist at this scale: successful implementations of thermal/shape memory [7,8], piezoelectric [9], dielectric elastomer [10,11], and (attractive-force) electrostatic [12–15] planar actuators have all been demonstrated, and the merits of each have been comprehensively discussed [16,17]. Electrostatic actuators have the benefits of operating with larger displacements than piezoelectric actuators and higher speeds than thermal/shape memory actuators, and are well-suited for planar manufacturing. We focus specifically on repulsive-force electrostatic actuators, due to advantages in stability, controllability, and reliability over other electrostatic actuators.

In this paper, we demonstrate a new electrode geometry for planar repulsive-force electrostatic actuators (RFA) – see Fig. 1 – that operates with increased forces, displacements, and field strengths as compared to existing RFA designs. Our new RFA is simulated to establish performance bounds, fabricated using a flex-circuit planar manufacturing process, and characterized as the driving actuator in one degree-of-freedom linear and rotational systems.

2. Background

Electrostatic actuators typically consist of sets of moveable electrodes (conductive plates or combs) separated by an insulating dielectric, with electrostatic forces proportional to the charge accumulation on and electric fields between electrodes due to an applied electric potential. Operation of all electrostatic actuators is limited by electrical breakdown (shorting), which occurs when the electric field strength between electrodes exceeds the dielectric strength of the insulating medium ($3–110 \times 10^6$ V/m in air and $154–303 \times 10^6$ V/m in polyimide) [24–27]. A comparison of meso-scale electrostatic actuators is provided in Table 1.

At μm-scales, parallel plate actuators use electrodes arranged in pairs of parallel plates [28], and comb drive actuators use a pair of interdigitated combs [29]. To actuate, an applied volt-

* Corresponding author.
E-mail address: ronf@eecs.berkeley.edu (R.S. Fearing).
URL: http://robotics.eecs.berkeley.edu/ronf/ (R.S. Fearing).

https://doi.org/10.1016/j.sna.2017.12.054

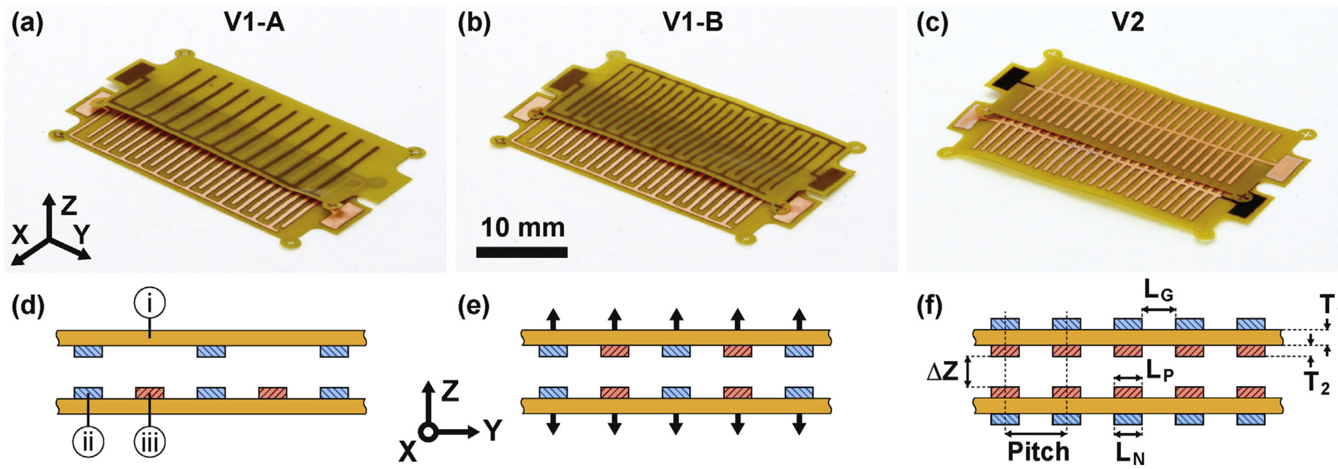

Fig. 1. Flexible, two-layer repulsive force actuator designs evaluated in this work: (a) V1-A, the electrode design used by S. He et al. [18], (b) V1-B, an improved design proposed by S. He et al. [19], (c) V2, the electrode design used in this work. For each actuator electrode design, the two functional layers are photographed (a–c) and the cross-sections are illustrated (d–f). Each actuator layer is composed of a polyimide substrate (i) with negative (ii) and positive (iii) electrodes. Actuator layers experience a net repulsive electrostatic pressure, illustrated in (e). Actuator dimensions include the substrate (T_1 = 25 μm) and electrode (T_2 = 18 μm) thickness, positive (L_P = 500 μm) and negative (L_N = 500 μm) electrode width, gap between adjacent electrodes (L_G = 500 μm), and inter-layer height (ΔZ).

age draws the electrodes together for gap-closing operation. To improve stroke length, the actuator output is often coupled to an inchworm mechanism [21]. At mm-scales, integrated force arrays [22,30] and distributed electrostatic actuators [12] are massively-parallelized actuators with 100s–1000s of connected parallel plate electrode units. Actuators at this scale are micro-fabricated, have high force density, low strains, and the highly-parallelized designs have low yields [30].

At cm-scales, dielectric elastomer actuators (DEA) use compliant electrodes fabricated on each side of low modulus elastomer film [20,31,32]. DEAs generate large strains (60%) and high pressures (100s kPa) during operation: applied voltages thin the elastomer (distance between the electrodes) and stretch the cross-sectional area. DEAs also exhibit significant viscoelastic behavior due to the compliant elastomer film. Gap-closing distributed electrostatic actuators [12], stacked electrostatic actuators [13], and zipper electrostatic actuators [14] generate mm to cm strokes, sub-N forces, and 100s Pa pressures. Linear surface-drive electrostatic film actuators [23] and motors [33] are flex-circuit devices that generate up to 4.4 N forces and 100s Pa pressures.

Repulsive force electrostatic actuators (RFA) are a subset of electrostatic actuators that generate a net repulsive force (instead of attractive force) through clever configuration of the 2+ sets of differentially polarized electrodes [33]. Similarly charged electrodes oppose one another on moveable layers to generate the inter-layer repulsive force. Oppositely charged electrodes establish the electric fields and potential gradients in the actuator, but minimize attractive forces between moveable layers by: spacing oppositely-charged electrodes further apart than like-charged electrodes to produce weaker out-of-plane attractive forces, using symmetry to minimize in-plane attractive forces, and having attractive forces act as internal body forces on noncompliant substrates.

RFAs in general have low complexity, generate peak force at the initial displacement, have linear or rotational outputs based on suspension design (minimizing transmission requirements), and avoid many common failure modes of electrostatic actuators – RFAs have no pull-in limit, no increased likelihood of breakdown as electrodes displace normally, and no stiction problem.

RFAs were first reported by W. Tang et al. [33]: electrodes patterned below a comb drive linear lateral resonator were used as

Table. 1
Survey of meso-scale electrostatic actuators, with key normalized metrics highlighted in grey.

Design	A / mm x mm	L / mm	ΔL / mm	ε / %	E / V/m	F / N	F/A / N/m²	BW / Hz	Source
Dielectric Elastomer	0.070 x 18	21	–	+61*	$43\cdot10^{6}$*	0.75	$600\cdot10^{3}$	15	[20]
Parallel Plate Inchworm	0.040 x 1.56	0.97	0.124	+13	$21\cdot10^{6}$	$2.23\cdot10^{-3}$	$1.38\cdot10^{3}$	39*	[21]
Integrated Force Array	0.002 x 1	10	0.700	-7.0	$80\cdot10^{6}$	$62\cdot10^{-6}$	$28\cdot10^{3}$	–	[22]
Stacked Electrostatic	54 x 54	2.27	0.420	-20.5	$28\cdot10^{6}$	1.27	435	–	[13]
Electrostatic Film Slider	50 x 100	0.380	–	–	$14.3\cdot10^{6}$	4.4	880	–	[23]
Distributed Electrostatic	0.005 x 4	5	0.028	-0.6	$33\cdot10^{6}$	$6.3\cdot10^{-6}$	315	1.6*	[12]
Distributed Electrostatic	31 x 28	11	4	-36	$5\cdot10^{6}$	–	–	–	[12]
Zipper Electrostatic	50 x 10	18.1	18	-99*	$110\cdot10^{6}$	–	–	12	[14]
Repulsive Force	3.26 x 3.26	0.004	0.086	+2000	$3.8\cdot10^{6}$	$5\cdot10^{-6}$*	2.9*	80-200	[18]
V1-A	80 x 10	0.136	–	–	$2\cdot10^{6}$	$2.74\cdot10^{-3}$	3.4	–	This Work
V1-B	25 x 10	0.136	–	–	$2\cdot10^{6}$	$1.04\cdot10^{-3}$	4.2	–	
V2	25 x 10	0.431	0.511	**+119**	$40\cdot10^{6}$	$9.03\cdot10^{-3}$	**36.1**	**43**	

A – area (orthogonal to stroke axis); L – length (parallel to stroke axis); E – electric field strength; ΔL – stroke length; ε – strain ($\Delta L/L$, with + indicating expansion); F – force; F/A – area force density; BW – frequency bandwidth. (*) denotes properties calculated from provided information.